PAGEOPH, Vol. 130, No. 4 (1989) 0033-4553/89/040617-18$1.50 + 0.20/0

Temporal Variation of Coda Q During Hualien Earthquake of 1986 in Eastern Taiwan

J. H. WANG[1], T. L. TENG[2] and K. F. MA[1]

Abstract—The May 20, 1986, Hualien earthquake sequence occurred on the northeastern coast of Taiwan. The $M = 6.1$ (GS mb) mainshock was followed by a large number of closely-clustered aftershocks with the largest being an $M = 5.5$ event. One seismic station, TWD of the Taiwan Telemetered Seismographic Network, is located in the surface projection of the source region and provides excellent recordings of the entire earthquake sequence. These recordings, plus events occurring in the same source area preceding the mainshock, offer a unique opportunity to study the spatial and temporal variations of coda Q in a region of active subduction. A simple technique is devised that uses the envelope of the coda waveform to enable a quick determination of the coda Q from drum records. For recordings with a peak power at about 8 Hz, the following findings have been obtained: 1. The ambient coda Q near an active subduction region was as low as 145; 2. There was no significant decrease in coda Q within the period beginning one year and four months prior to the mainshock; 3. There was a significant drop of coda Q immediately after the mainshock; this drop lasted approximately two days before returning to the ambient level; 4. Coda Q values varied with focal depth.

Key words: Coda Q, envelope decay curve, temporal variation.

Introduction

The application of statistical techniques to high-frequency seismic recordings has resulted in the study of coda waves. The interpretation of the decay of the coda amplitude in terms of a backscattering theory was pioneered by AKI (1969). Subsequent theoretical developments and measurements on the coda portion of the seismogram have yielded important structural information about the lithosphere (AKI and CHOUET, 1975; CHOUET, 1976; KOPNICHEV, 1977; RAUTIAN and KHALTURIN, 1978; CHOUET *et al.*, 1978; TSUJIURA, 1978; AKI, 1980a,b; SATO, 1977, 1978, 1979, 1984; WU, 1984; GUSER and LEMZIKOV, 1985). From the measurement of the coda decay, an estimate of high-frequency attenuation of seismic waves,

[1] Institute of Earth Sciences, Academia Sinica, P.O. Box 23-59, Taipei, Taiwan, 10764, R.O.C.
[2] Department of Geological Sciences, University of Southern California, Los Angeles, CA 90089-0740, U.S.A.

referred to as the coda Q, is obtainable for regions sampled by backscattering waves (HERRMANN, 1980; SINGH and HERRMANN, 1983).

Both spatial and temporal variations of coda Q have been examined. Notably, AKI and CHOUET (1975) found that the coda decay rate is much faster in a tectonically active region than in a stable region. SINGH and HERRMANN (1983) mapped the coda Q of the United States and presented a contour map that substantiates AKI and CHOUET'S findings. They showed that the continental United States in the region of the Rocky Mountains has a much lower coda Q than the region east of it, and that the general distribution of coda Q correlates with the local tectonic stability. SHIN *et al.* (1987) have estimated the coda Q value of the Taiwan region to be from 120 to 300 at 2 Hz, with a value of 150 in the Hualien area; these values are comparable to those found by SINGH and HERRMANN (1983) for the Pacific coast region of the United States. CHOUET (1979) studied the temporal variation of the coda attenuation near Stone Canyon, California, and found a strong indication of coda Q changes with time. A number of investigations (JIN, 1981; NOVELO-CASANOVA *et al.*, 1985 TSUKUDA, 1985; JIN and AKI, 1986; LEE *et al.*, 1986; PENG *et al.*, 1987) have found significant changes in coda Q before large earthquakes. The relevance of these findings to earthquake prediction is obvious.

To further examine the temporal variation of coda Q before and after a large earthquake, we make use of a well-localized seismic source region in Taiwan that frequently emits a large number of events which are well-recorded at a nearby station. A large $M = 6.1$ earthquake occurred in this source region on May 20, 1986 with numerous aftershocks (CHEN and WANG, 1986). This large body of data is used to examine the temporal variation of coda Q before and after the mainshock. In order to minimize the effects of the source function and path propagation on the coda Q, we have confined the events used in this study to be in the magnitude range of $2.5 < M < 3.0$ and within a cubic volume of approximately 20 km on each side. This subset includes over 125 excellent aftershock records. Seismograms are recorded by station TWD of the Taiwan Telemetered Seismographic Network (TTSN). This station is located practically in the center of the surface projection of the source region. This geometry approximates the assumptions of the single isotropic scattering theory of SATO (1977) and makes the ellipsoidal sampling volumes for all source points largely overlapping. Thus, the obtained coda Q should reflect the property of the medium in the proximity of the source region.

Data

A magnitude 6.1 (GS mb) earthquake occurred on May 20, 1986 at 05 : 25 GMT on the northeastern coast of Taiwan, a location where the Philippine Sea plate is known to have been subducting underneath the Eurasia continent along the west-trending Ryukyu trench (TSAI *et al.*, 1977). The mainshock, as located by the

TTSN, is placed at 24.08°N, 121.59°E, and at a depth of 15.8 km. Its aftershocks are located within a small region of 10 km in radius with the mainshock epicenter and one of the TTSN stations, TWD, located almost in the center of the region (Figure 1). A large number of aftershocks followed; more than 500 events occurred with the first five days. Only events of magnitude 2.5 to 3.0 and inside the dashed rectangle of Figure 1 are used in the present analysis. The great majority of the events are within a cubic volume 20 km on each side. The chosen magnitude range insures on-scale recording and a homogeneous coverage. The spatial limits define the sampling volume from which coda Q information is sought; the narrow magnitude range confines the source excitation to an approximately uniform frequency band. Within the magnitude range and spatial limits, a data set of 125 events is obtained for the present study. We have also collected all foreshocks in the same source volume for the period of one year and four months preceding the mainshock. Relevant information of the complete data set used is given in Table 1. The aftershocks form two clusters, which show a distinct separation that can be seen along a northwest-southeast cross-section SS′ shown in Figure 2. The western cluster is associated with a SE-dipping fault that is well-defined by the aftershocks.

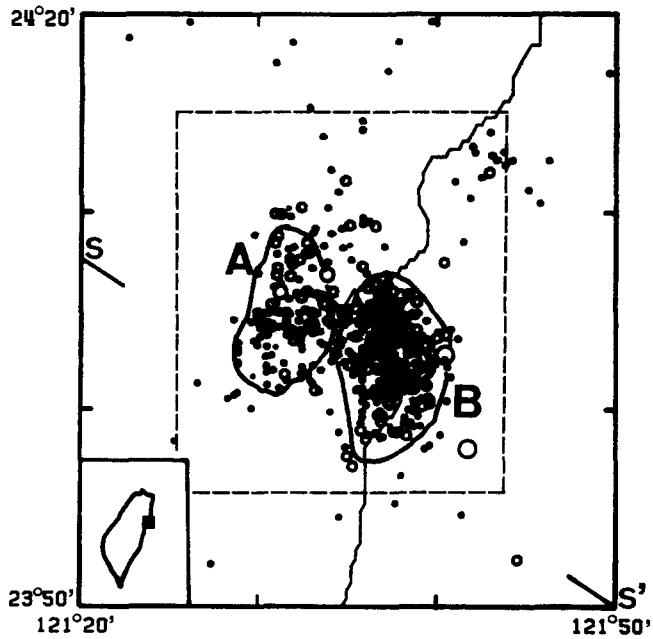

Figure 1
Epicentral distribution of the May 20, 1986 mainshock (shown by a open star), aftershocks in two cluster: Group A for onland events and Group B for offshore events (after CHEN and WANG, 1986). Station TWD is shown by an open triangle. Circles of different sizes denote earthquakes of different magnitudes.

Table 1

Listing of earthquakes used and the estimated Coda Q

No	Time						Lat.		Long.		Depth		
	Yr	Mo	Da	Hr	Mi	Sec	(°)	(′)	(°)	(′)	(km)	*M*	*Q*
1	85	1	22	20	10	51.0	24	.4	121	31.8	14.6	2.7	120
2	85	1	28	4	53	28.2	24	11.2	121	39.4	18.6	2.6	80
3	85	1	4	9	37	57.0	25	8.8	121	39.3	2.5	2.9	120
4	85	2	5	0	27	5.0	24	3.0	121	37.5	7.2	3.0	240
5	85	2	5	0	48	24.2	24	4.4	121	36.9	2.5	2.9	120
6	85	2	6	15	7	56.6	24	10.0	121	38.4	1.5	2.9	160
7	85	2	14	19	49	58.4	24	9.8	121	42.2	13.3	3.0	80
8	85	3	1	20	53	36.5	24	.2	121	36.3	7.6	2.9	240
9	85	3	1	20	53	34.4	24	2.3	121	35.8	1.6	2.8	120
10	85	4	1	6	45	4.5	24	4.9	121	38.4	28.7	2.9	80
11	85	4	12	9	8	7.8	24	5.9	121	41.5	24.6	3.0	120
12	85	4	12	20	34	3.5	24	7.0	121	37.7	18.6	3.0	120
13	85	5	16	18	13	47.5	24	15.0	121	40.0	24.0	2.9	160
14	85	6	1	8	16	55.8	24	8.0	121	32.2	28.5	2.8	40
15	85	6	11	8	25	23.7	24	7.8	121	35.8	22.1	2.7	40
16	85	7	5	9	52	33.9	24	2.5	121	37.4	88.5	2.6	200
17	85	7	8	2	31	24.5	24	10.2	121	34.1	16.7	2.7	160
18	85	7	11	20	32	23.7	24	9.1	121	39.7	5.2	2.8	160
19	85	7	13	20	8	55.1	23	55.5	121	43.4	21.0	2.6	40
20	85	7	14	16	48	11.5	23	59.1	121	36.8	7.6	2.5	120
21	85	7	19	23	46	.3	24	13.3	121	43.6	7.6	2.8	80
22	85	8	2	24	9	18.6	24	4.3	121	32.7	13.9	2.8	80
23	85	9	11	16	24	55.9	23	57.3	121	38.9	27.3	2.8	120
24	85	9	24	4	29	15.8	24	11.8	121	44.5	2.1	2.8	160
25	85	10	2	14	53	41.0	24	5.8	121	29.6	10.0	2.9	240
26	85	10	20	10	0	11.9	24	13.4	121	33.1	10.3	2.6	160
27	85	10	31	21	53	45.3	24	9.1	121	43.1	21.0	2.7	160
28	85	11	2	4	5	56.6	24	3.7	121	40.6	4.0	2.7	200
29	85	11	5	9	56	12.7	24	8.8	121	40.5	21.8	2.7	240
30	85	11	5	16	14	33.3	24	.4	121	39.9	15.7	2.9	240
31	85	11	13	9	55	31.2	24	13.9	121	43.6	8.7	2.2	240
32	85	11	15	9	8	51.2	23	55.7	121	28.7	8.3	2.7	120
33	85	11	16	10	47	4.5	24	3.7	121	26.2	7.3	2.6	120
34	85	11	27	15	43	34.3	24	1.1	121	26.8	8.3	2.7	80
35	85	11	30	16	44	24.2	24	9.4	121	31.7	2.9	2.8	240
36	85	12	17	11	30	5.4	24	4.9	121	30.9	23.0	2.6	40
37	86	1	18	18	52	9.1	24	10.1	121	43.7	10.1	2.7	240
38	86	1	27	4	21	35.1	24	10.3	121	43.7	7.7	2.5	160
39	86	1	22	14	37	31.4	24	8.0	121	40.1	15.8	2.5	120
40	86	1	22	15	23	53.5	24	10.4	121	43.8	6.2	2.6	160
41	86	1	23	6	21	26.7	24	8.1	121	39.8	14.9	2.5	240
42	86	1	24	8	58	55.0	24	9.5	121	44.2	12.2	2.9	80
43	86	1	24	9	38	9.4	24	11.4	121	42.7	6.7	2.9	120
44	86	1	27	18	25	35.1	24	11.8	121	42.3	8.1	2.7	160
45	86	2	3	2	58	6.7	24	7.5	121	43.4	13.4	2.6	40

Table 1 (*cont.*)

No	Time						Lat.		Long.		Depth		
	Yr	Mo	Da	Hr	Mi	Sec	(°)	(′)	(°)	(′)	(km)	*M*	*Q*
46	86	2	4	3	31	16.1	23	57.2	121	40.6	21.5	2.8	80
47	86	2	9	5	43	7.3	24	6.4	121	32.1	15.4	2.6	120
48	86	2	9	12	44	13.6	24	5.5	121	40.9	25.7	3.0	160
49	86	2	11	21	56	6.6	24	2.9	121	34.4	14.0	3.0	240
50	86	2	28	16	40	46.5	23	58.9	121	29.1	6.6	2.8	240
51	86	3	1	17	47	15.8	24	8.4	121	35.9	27.9	2.9	160
52	86	3	9	9	29	57.1	24	12.2	121	38.0	.6	2.6	120
53	86	3	19	10	31	59.8	24	12.6	121	44.5	25.6	2.6	120
54	86	3	29	0	11	57.7	24	14.1	121	34.7	2.2	2.5	160
55	86	3	7	8	4	17.8	24	.6	121	36.9	6.2	2.7	40
56	86	5	10	9	18	1.9	24	10.0	121	43.7	6.6	2.9	160
57	86	5	14	6	42	27.1	24	14.7	121	40.2	2.8	2.6	80
58	86	5	20	5	51	21.9	24	1.9	121	30.5	14.3	2.6	160
59	86	5	20	7	15	51.1	24	3.6	121	37.1	17.6	2.6	80
60	86	5	20	10	1	28.2	24	3.4	121	33.5	16.4	2.9	160
61	86	5	20	10	20	27.8	24	5.9	121	33.1	15.7	2.6	80
62	86	5	20	10	25	34.7	24	3.9	121	34.4	4.6	2.6	120
63	86	5	20	10	58	43.7	24	3.8	121	33.1	17.1	2.9	160
64	86	5	20	14	27	18.7	24	3.6	121	32.4	17.6	2.9	160
65	86	5	20	14	30	26.1	24	13.1	121	43.8	3.3	3.0	160
66	86	5	20	15	2	17.3	24	2.0	121	33.5	17.6	2.9	160
67	86	5	20	15	8	17.8	24	4.1	121	30.9	14.0	2.5	160
68	86	5	20	16	22	55.2	24	1.5	121	31.6	16.4	2.7	120
69	86	5	20	16	26	56.5	24	11.6	121	41.1	11.1	2.5	160
70	86	5	20	17	58	6.9	24	4.9	121	33.3	15.6	3.0	240
71	86	5	20	19	21	15.5	24	4.4	121	33.1	15.7	2.9	160
72	86	5	20	19	52	58.3	24	1.9	121	38.1	14.4	2.8	160
73	86	5	21	4	48	11.7	24	4.5	121	33.8	19.6	2.8	80
74	86	5	21	7	24	8.9	24	.5	121	36.7	6.3	2.7	80
75	86	5	21	7	57	20.2	24	10.7	121	41.9	9.9	2.6	120
76	86	5	21	10	23	24.1	24	5.9	121	32.2	14.1	2.6	80
77	86	5	21	11	41	26.2	24	7.3	121	35.8	17.6	2.0	120
78	86	5	21	11	42	6.3	24	5.6	121	31.8	15.7	2.7	80
79	86	5	21	14	24	36.3	24	4.0	121	31.6	17.2	2.8	80
80	86	5	21	14	50	11.9	24	1.2	121	38.5	6.4	2.9	80
81	86	5	21	14	56	17.5	24	.9	121	38.0	6.4	2.8	80
82	86	5	21	15	10	35.1	24	1.5	121	38.9	5.6	2.7	80
83	86	5	21	17	41	11.1	23	58.8	121	37.5	5.1	2.9	40
84	86	5	21	17	43	55.1	23	59.9	121	34.1	14.9	2.9	120
85	86	5	21	17	44	53.8	24	2.4	121	34.9	12.6	2.7	80
86	86	5	21	17	48	28.4	24	2.0	121	37.2	3.0	2.7	120
87	86	5	21	18	12	58.2	24	1.2	121	30.5	14.8	2.9	80
88	86	5	21	18	31	46.6	24	1.1	121	38.5	6.3	2.9	80
89	86	5	21	19	8	32.7	24	7.5	121	33.9	15.9	2.6	80
90	86	5	21	19	32	59.3	24	8.3	121	37.1	12.9	2.6	80
91	86	5	21	19	33	16.7	24	6.9	121	37.2	15.1	2.6	120

Table 1 (*cont.*)

No	Time						Lat.		Long.		Depth (km)	M	Q
	Yr	Mo	Da	Hr	Mi	Sec	(°)	(′)	(°)	(′)			
92	86	5	21	19	35	19.0	24	.4	121	35.8	5.1	2.6	80
93	86	5	21	20	40	5.8	24	4.4	121	29.6	15.3	2.6	80
94	86	5	21	20	41	25.4	24	1.9	121	38.9	6.0	2.7	40
95	86	5	21	21	26	19.4	24	1.1	121	37.7	7.1	2.7	80
96	86	5	21	21	58	30.6	23	58.8	121	37.7	3.3	2.6	120
97	86	5	21	22	24	20.7	24	2.7	121	37.0	7.3	2.6	80
98	86	5	21	22	28	5.1	24	4.9	121	31.1	12.9	2.7	80
99	86	5	22	2	53	21.6	24	4.9	121	32.9	16.0	2.9	80
100	86	5	22	4	6	25.4	24	3.1	121	38.5	6.7	2.8	80
101	86	5	22	4	33	31.9	24	2.1	121	38.3	4.1	2.6	120
102	86	5	22	5	6	11.9	24	11.0	121	34.5	1.5	2.8	120
103	86	5	22	5	7	26.4	24	9.7	121	35.8	11.9	2.9	120
104	86	5	22	5	12	36.2	23	5.1	121	39.6	7.4	2.9	120
105	86	5	22	6	29	30.2	24	4.8	121	38.4	3.1	2.9	120
106	86	5	22	6	37	20.4	23	59.1	121	38.7	5.8	2.6	80
107	86	5	22	7	26	40.5	24	4.9	121	32.3	17.4	2.8	80
108	86	5	22	7	48	17.9	24	4.5	121	35.8	4.5	2.6	80
109	86	5	22	8	13	31.4	24	3.5	121	36.7	5.6	2.7	120
110	86	5	22	11	18	20.6	24	4.9	121	34.7	3.8	2.9	120
111	86	5	22	12	12	52.5	24	9.8	121	31.8	4.6	2.8	120
112	86	5	22	12	47	6.7	24	2.3	121	37.0	5.4	2.6	40
113	86	5	22	12	49	6.1	24	3.1	121	35.8	5.6	2.8	80
114	86	5	22	13	0	46.9	24	1.9	121	37.6	7.1	2.5	120
115	86	5	22	13	24	.4	24	3.3	121	36.1	6.4	2.6	160
116	86	5	22	13	30	32.5	24	4.4	121	35.6	2.0	2.7	120
117	86	5	22	15	23	2.8	24	1.9	121	36.7	6.1	2.7	80
118	86	5	22	16	23	21.1	24	7.9	121	32.6	12.1	2.9	80
119	86	5	23	1	1	12.4	24	2.3	121	38.8	3.4	3.0	160
120	86	5	23	2	0	20.9	24	.4	121	40.6	1.3	3.0	160
121	86	5	23	2	33	9.3	24	2.7	121	37.7	6.0	2.8	160
122	86	5	23	12	7	55.3	24	6.4	121	37.1	.8	2.9	160
123	86	5	23	15	38	51.7	24	.8	121	35.8	6.3	2.7	120
124	86	5	23	17	38	20.0	24	12.9	121	43.1	7.0	2.5	80
125	86	5	23	18	5	10.6	24	4.0	121	35.8	5.7	2.6	120
126	86	5	23	19	34	.6	24	3.6	121	38.3	6.1	2.9	160
127	86	5	23	19	40	50.1	24	3.9	121	37.0	6.3	2.7	160
128	86	5	23	23	34	10.3	24	15.2	121	35.8	15.7	2.6	80
129	86	5	24	4	35	36.8	24	4.6	121	38.3	3.7	3.0	160
130	86	5	24	4	36	32.4	24	5.6	121	36.6	4.2	2.6	160
131	86	5	24	4	43	19.6	24	4.6	121	37.8	5.1	2.7	120
132	86	5	24	8	45	35.9	24	3.7	121	36.4	4.1	2.8	240
133	86	5	24	8	56	50.4	23	59.6	121	35.8	5.1	2.6	160
134	86	5	24	10	9	29.6	24	.7	121	37.1	3.4	2.9	160
135	86	5	24	10	11	29.9	24	1.9	121	39.6	2.6	2.9	160
136	86	5	24	10	30	47.0	24	2.2	121	35.8	3.8	2.6	160
137	86	5	24	10	40	53.0	24	.6	121	37.4	6.9	2.7	120

Table 1 (*cont.*)

No	Time						Lat.		Long.		Depth		
	Yr	Mo	Da	Hr	Mi	Sec	(°)	(′)	(°)	(′)	(km)	*M*	*Q*
138	86	5	24	10	43	.5	24	1.1	121	35.8	6.5	2.7	160
139	86	5	24	11	34	37.4	23	58.6	121	37.0	2.7	2.7	80
140	86	5	24	16	13	50.8	24	4.1	121	37.2	5.7	2.6	160
141	86	5	24	17	55	27.7	23	58.0	121	34.9	2.5	2.9	240
142	86	5	24	18	15	15.7	24	3.2	121	38.9	1.3	2.7	160
143	86	5	24	18	27	36.4	24	.0	121	29.6	11.3	2.6	160
144	86	5	24	18	45	33.4	24	1.8	121	39.9	1.2	2.9	240
145	86	5	24	21	31	52.3	24	4.9	121	39.0	2.8	2.0	240
146	86	5	24	21	50	44.3	24	2.8	121	35.2	6.2	2.7	120
147	86	5	24	21	52	11.9	24	1.4	121	37.5	3.2	2.9	240
148	86	5	24	22	4	44.0	24	4.1	121	38.0	3.2	2.6	80
149	86	5	24	23	8	37.0	24	5.0	121	34.4	3.9	2.9	320
150	86	5	24	23	38	52.9	24	1.1	121	31.2	15.4	2.7	120
151	86	5	24	23	42	22.3	24	.4	121	39.1	1.5	2.7	160
152	86	5	24	23	53	.7	24	6.8	121	31.8	9.1	3.0	240
153	86	5	25	6	53	3.6	24	3.3	121	30.4	16.2	2.7	80
154	86	5	25	7	6	5.8	24	4.9	121	30.8	14.4	2.5	80
155	86	5	25	10	44	3.7	24	8.7	121	31.7	3.3	2.9	240
156	86	5	25	22	39	43.7	24	5.0	121	31.3	17.9	2.6	80
157	86	5	26	3	0	34.5	24	6.1	121	33.8	8.3	2.7	120
158	86	5	26	4	47	59.6	24	9.1	121	35.3	14.6	2.6	40
159	86	5	26	9	18	6.2	24	8.4	121	37.4	18.3	2.7	40
160	86	5	26	9	48	39.0	24	3.2	121	38.0	5.8	2.7	40
161	86	5	26	10	32	37.0	24	4.9	121	36.6	5.4	2.7	40
162	86	5	26	11	25	16.8	24	4.9	121	36.6	5.1	2.6	40
163	86	5	26	19	35	54.3	24	4.9	121	32.8	10.6	2.8	80
164	86	5	26	23	32	22.1	24	3.7	121	40.1	4-1	2.7	80
165	86	5	27	19	39	56.0	24	5.3	121	43.3	6.7	2.9	240
166	86	5	28	3	11	19.0	24	3.1	121	37.9	3.9	2.8	160
167	86	5	28	3	43	52.4	24	4.4	121	36.1	10.1	2.7	120
168	86	5	28	16	5	24.5	24	7.8	121	36.3	17.4	2.9	160
169	86	5	28	21	32	28.9	24	.6	121	37.0	5.0	2.6	80
170	86	5	29	1	8	21.7	24	1.2	121	33.6	17.9	2.7	160
171	86	5	29	4	46	33.9	24	1.7	121	41.4	13.8	3.0	160
172	86	5	29	7	2	9.2	24	9.9	121	38.8	9.8	2.5	160
173	86	5	29	7	29	13.6	24	2.2	121	35.8	5.9	2.7	160
174	86	5	29	19	55	42.4	23	58.5	121	37.7	1.1	3.0	240
175	86	5	30	5	1	45.4	23	58.9	121	31.3	1.4	2.5	80
176	86	5	30	12	50	33.4	24	2.9	121	39.1	6.4	2.7	240
177	86	5	30	16	5	17.4	23	59.2	121	43.3	8.4	2.6	80
178	86	5	30	20	57	32.6	23	58.2	121	36.7	.7	2.8	160
179	86	5	31	6	55	18.1	23	57.7	121	35.8	5.4	2.8	240
180	86	5	31	7	0	28.5	23	59.8	121	36.7	2.7	2.7	240
181	86	5	31	8	28	36.2	24	2.6	121	38.6	4.7	2.6	160
182	86	5	31	15	36	20.3	34	3.1	121	33.8	16.6	3.0	320

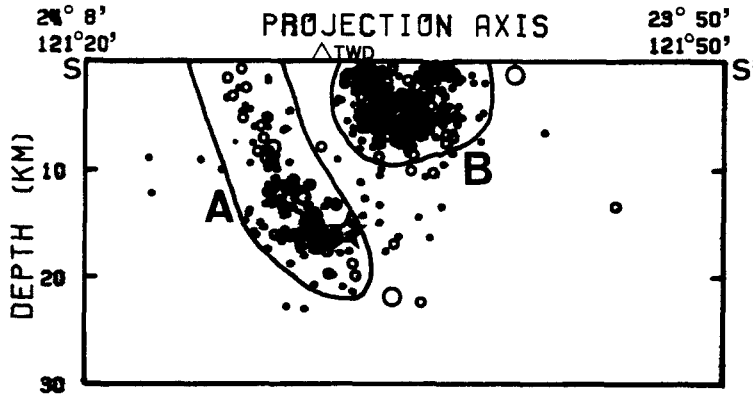

Figure 2
Cross-section along SS′ of Figure 1 (after CHEN and WANG, 1986).

The eastern cluster is associated with several parallel thrust faults of similar nature, but the events are shallower in depth. One of the shallow faults in the eastern cluster is well-known for its surface rupture during the strong earthquake in 1951 (HSU, 1954). Fourteen hours after the mainshock, a temporary network of 3 stations was set up in the source region; the number of stations increased to 11 in three days and offered excellent control in hypocenter location and fault-plane determination (LIAO *et al.*, 1986). A thrust fault mechanism is found for both the mainshock and the aftershocks with strike N 35°E and dip 60°SE this solution is consistent with the aftershock distribution shown in Figure 2. Recordings of this earthquake sequence are well suited for a coda Q study because the seismic station TWD is located practically directly above the source region. This minimizes waveform complications due to the path. Events used in our measurements have very similar waveforms that are characterized by an exponential decay of the S-coda. The rate of decay gives a measure of the parameter defined as the coda Q in the next section.

Method of Coda Q Measurement

For single isotropic scattering of short-period body waves, SATO (1977) expressed the mean energy density of scattered waves at frequency ω by the following formula:

$$E(r, t, \omega) = (n\sigma W/4\pi r^2)K(t/t_S) \exp(-\omega t/Q), \quad t > t_S \tag{1}$$

where r is the distance between the source and the receiver, t is the lapse time measured from the origin time, W is the total radiated energy density in a narrow band with center frequency ω, $n\sigma$ is the effective scattering coefficient, Q is the

apparent quality factor that combines the effects of scattering and inelastic absorption, t_S is the travel time of S waves and

$$K(t/t_S) = (t/t_S) \ln[(t + t_S)/(t - t_S)]. \quad (2)$$

Both the primary waves and the scattered waves are assumed to be S waves. To measure the coda Q in (1), we follow JIN and AKI (1986) by estimating the energy density from the amplitude measured directly on a seismogram. For a seismogram written by a short-period narrow band instrument with center frequency ω, the energy density ratio $E(r, t|w)/E_S(r|\omega)$ can be approximated by the amplitude ratio square $[A(t)/A_S]^2$. $A(t)$ is the mean amplitude of the coda waves around the lapse time t; and A_S is the maximum amplitude of S waves. The energy density of direct S waves from a point source with a short source duration u is:

$$E(r/\omega) = W/(4\pi r^2 \beta u) \exp(-\omega t_S/Q). \quad (3)$$

Taking the ratio of (1) and (3), we get:

$$A(t) = CA_S K(t/t_S) \exp[-\omega(t - t_S)/2Q], \quad (4)$$

where $C = (n\beta\sigma u)^{1/2}$ is approximately independent of the lapse time. $A(t)$, as given by (4), is an exponential function of the coda envelope that is strongly dependent on Q. $A(t)$ is then used to extract coda Q information by applying it to the analog data described below.

To apply Eq. (4) we use only small earthquakes to ensure that the source excitation function u is short and not too variable so that its influence on the coda envelope is insignificant. From the large number of events, we further confine the data used to be within the magnitude range $M = 2.5$ to 3.0, to insure high enough signal-to-noise ratio yet with on-scale S-wave amplitude. Normally, waves in the interval 20 to 30 sec after the S arrival are used to determine the decay rate.

Station TWD is equipped with both vertical and horizontal seismometers (Kinemetrics SS-1) of 1 Hz natural frequency. The overall instrumental response of the TTSN is given in Figure 3. Velocity is recorded on the drums and the flat portion of the velocity response ranges from 2 to 10 Hz. We have checked the dominant frequency of the recorded coda waves in two ways. First, we have used digital recordings that became available for the TTSN in 1987. Coda wave spectra were obtained for a few small ($M = 2.5$ to 3.0) events from the same source area in which digital recordings were made. These power spectra show a dominant peak at about 8 Hz. Second, the dominant frequency derived from zero-crossings on the coda portion of the drum records also confirms the 8 Hz estimate. Although Eq. (4) is for the band-passed displacement at center frequency ω when applied to velocity signals recorded by a narrow band system, the extra factor of frequency is absorbed by the constant C.

Based on Eq. (4), families of envelope decay curves as functions of lapse time are computed. A few sets of these decay curves are shown in Figure 4 for various

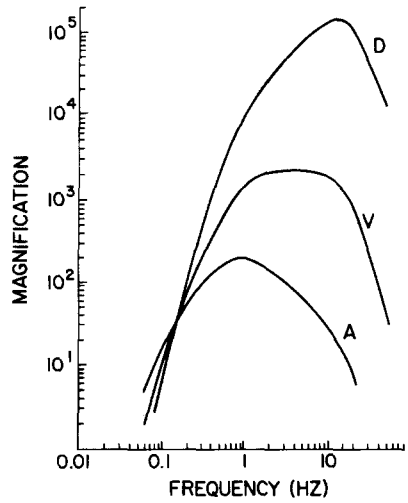

Figure 3
The response curves of the TTSN velocity-type sensor: 'A' for acceleration, 'V' for velocity, and 'D' for displacement.

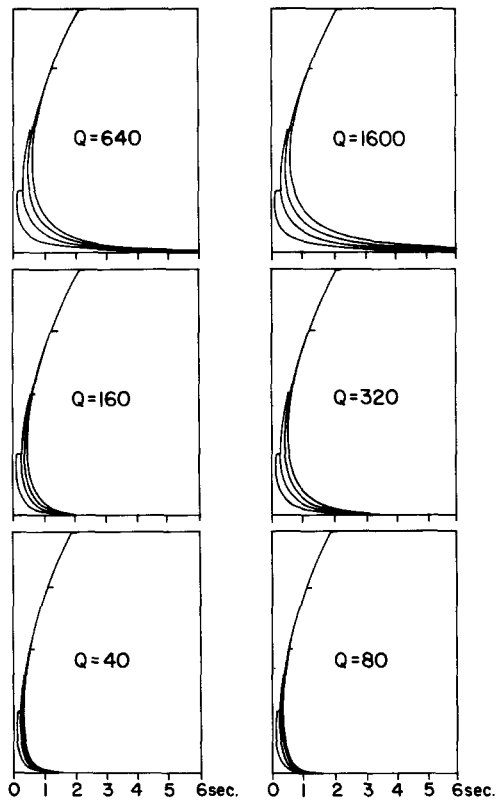

Figure 4
Sample envelopes of various c values and an S-wave lapse time of 4 sec for coda Q equal 40 to 1600 in increments of two.

values of Q and C. In this computation, a transformation is applied to the wave amplitude so that curvilinear motion of the recording pen of finite arm length (15 cm) can be taken into account. The family of decay curves is overlain on the recorded coda waves and a coda Q value can be directly read from the drum record. This procedure can be applied to either vertical or horizontal seismograms. Since the S-wave arrival is much clearer on the horizontal component, the coda Q measurements reported here are derived from the horizontal seismograms recorded at TWD. This procedure gives an approximate estimate of coda Q from graphic matching of seismograms to the envelope decay curves. It provides adequate resolution for the temporal variations on coda Q described later.

Coda Q: Temporal Variation and Depth Dependence

Temporal variations of coda Q values for foreshocks between January 1, 1985 to May 19, 1986 are shown in Figure 5a, and coda Q values for aftershocks from May 20 to 31, 1986 are shown in Figure 5b. All events plotted are located inside the source volume with the same narrow magnitude range from $M = 2.5$ to 3.0. The coda Q values for foreshocks vary from 40 to 240 with a mean of 141 and a standard deviation of 39. This average value is similar to that determined by SHIN *et al.* (1987). Their values are derived from the later portion of the coda waves of 4 events, with frequency ranging from 0.7 to 6 Hz. Our coda Q values are obtained mainly from the entire decay envelope after the S waves, with an estimated dominant frequency of 8 Hz. With the available data density, Figure 5a shows no clear indication of decrease of coda Q prior to the mainshock. Figure 5b gives detailed variations of coda Q for 125 aftershocks over a period of 12 days after the occurrence of the mainshock. The overall mean and standard deviation of the measured coda Q (130 ± 37) are practically the same as those for the foreshocks. However, a close examination of the data distribution shows certain rather well-defined changes that can be grouped into 5 intervals:

(1) May 20, coda $Q = 149 \pm 24$. Immediately following the mainshock, the measured coda Q values from 15 aftershocks maintain about the same background level as the foreshock period.

(2) May 21–22, coda $Q = 93 \pm 16$. This drop is clearly defined by 46 events for the entire two days.

(3) May 23–25, coda $Q = 156 \pm 37$. The value seems to return to the background level as determined from 38 measurements.

(4) May 26, coda $Q = 84 \pm 40$. This second drop may or may not be very reliable as it is determined by only 9 measurements with a larger standard deviation.

(5) May 27–31, coda $Q = 171 \pm 41$. Again, the value returns to the background level or perhaps somewhat higher.

The most interesting observation on the temporal variations of coda Q is the sharp drop in time interval (2). Defined by a large number of events, this drop

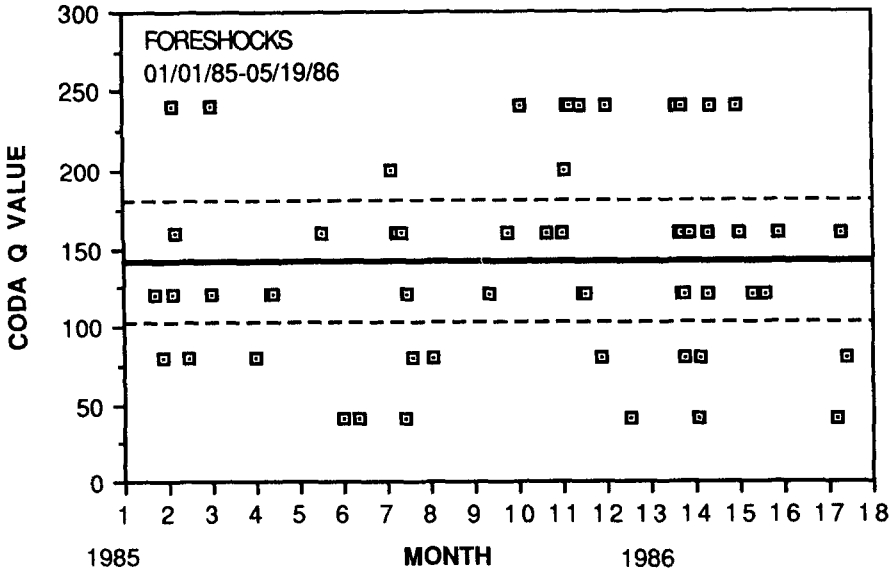

Fig. 5(a)

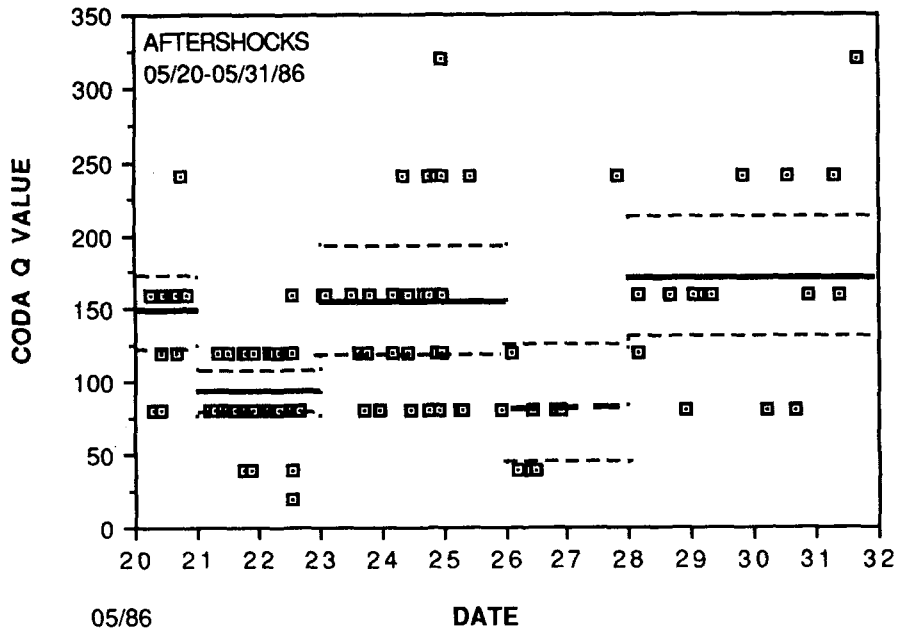

Fig. 5(b)

Figure 5

Temporal distribution of coda Q before and after the mainshock: (a) for foreshocks during January 1, 1985 to May 19, 1986 (in unit of month); and (b) for aftershocks in the studied area (in unit of day from May 20–31, 1986). The means and standard deviations of coda Q values in various time intervals are shown by the solid and dashed lines, respectively.

cannot be explained by the fact that more aftershocks during this interval originated from a particular depth range, as almost all the events in time interval (3) occurred at a similar depth range, yet they give a substantially higher coda Q.

It is interesting to determine whether the temporal variations of coda Q are dependent on the spatial distribution of the aftershocks, *i.e.*, whether they are obtained from group A or from group B as defined in Figures 1 and 2, or if they are dependent on focal depth. Figure 6a gives the distribution of coda Q values as a function of focal depth for the complete set of events. The solid line is for foreshocks and the dashed line is for aftershocks. For both cases, one can see a general decrease of coda Q with focal depth. The drop of coda Q for aftershocks is particularly pronounced for depths below 5 km; on the other hand, a small increase in coda Q for aftershocks is seen above the 5 km depth level. The solid curve and the dashed curve in Figure 6a bracket a depth range of 5 to 20 km in which the overall coda Q values show a significant drop. It appears that coda Q measurements can be used to obtain a measure of the source volume, and the degree of coda Q drop in this volume may indicate the intensity of the rupture process. Here, we recognize that the relative contribution of scattering and anelasticity to the measured apparent attenuation of coda waves remains an outstanding problem, as the two processes are not easily separable. If scattering is caused by inhomogeneities in terms of variations of microcrack density in a medium, then the generation of new cracks would tend to increase the wave scattering and thus lengthen the coda waves which leads to a larger value of coda Q. On the other hand, the new cracks are not likely to be dry, rather they are more likely to be fluid-filled. Wave energy would be absorbed by the motion of the fluid in the cracks causing a decrease of intrinsic Q. The consequence of lower intrinsic Q would shorten the length of the wavepath, thus reducing the effect of the scattering process. There is evidence pointing to the argument that the coda decay rate is more sensitive to the intrinsic Q, and much less so to the scattering. The agreement of coda Q and Q_β measurements (AKI, 1980b) is an example. In a numerical simulation study, FRANKEL and WENNERGERG (1987) also show a strong dependence of coda decay rate on the intrinsic Q of the medium. By applying their model to earthquake data from Anza, California, they further conclude that the measured coda Q does not relate to the scattering Q. We thus postulate that the generation of fluid-filled cracks following the occurrence of an earthquake would be the principal cause leading to a lower intrinsic Q and causes a steeper coda decay. Since the maximum drop of coda Q occurs in the 5 to 15 km depth interval, this suggests that extensive fracturing or crack-opening has taken place within this depth range during the aftershock sequence. Figure 6b gives a plot for the number of events in separate depth intervals from which coda Q values are determined. The small increase in coda Q after the main shock for the uppermost 5 km is determined by a large number of events; most of these events come from the shallow portion of the group B aftershocks. It is possible that, before the occurrence of the mainshock, compressive stress was building up along the fault

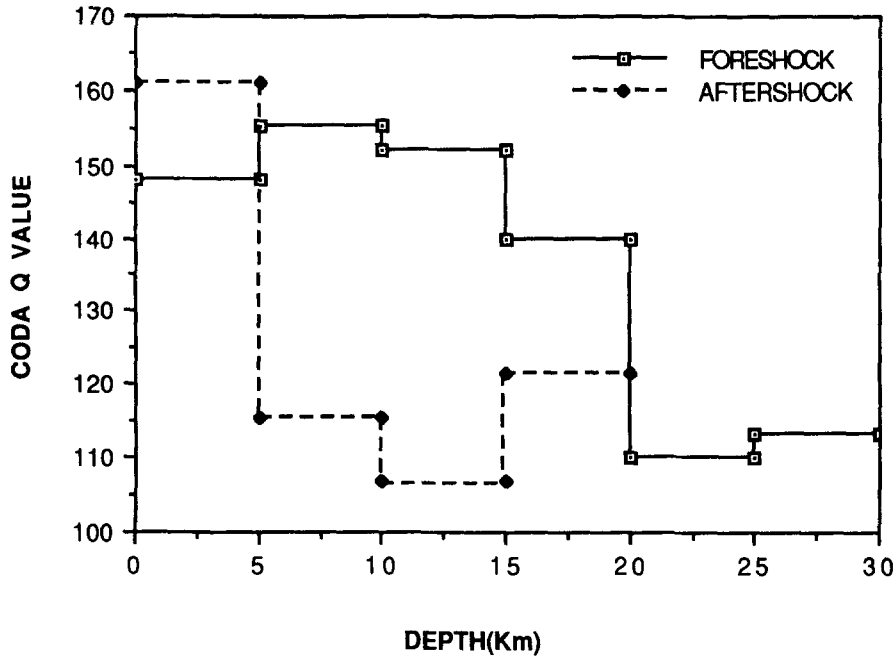

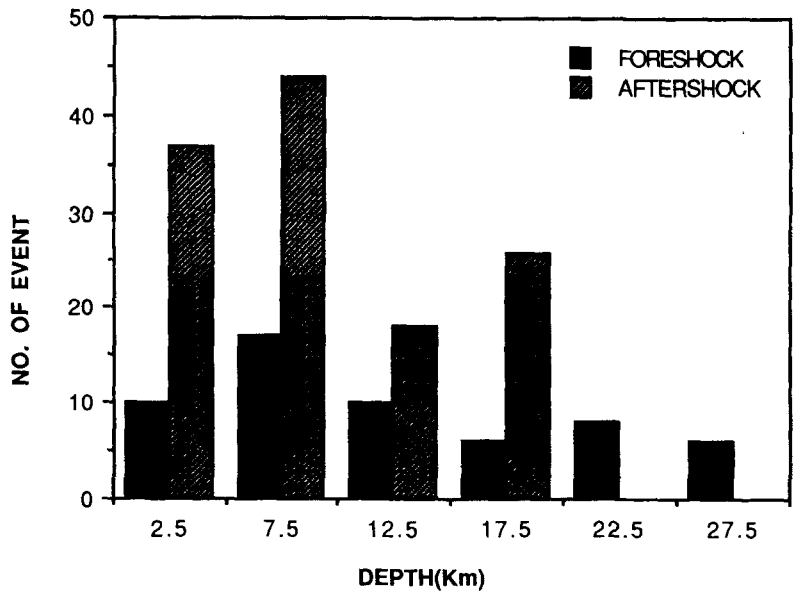

Figure 6
(a) Changes of coda Q before and after the mainshock as a function of focal depth; and (b) number of events in depth intervals from which coda Q values are determined.

zone, which eventually ruptured to first generate the group A aftershocks. Afterwards, the compressive stress shifted to that part of the source volume eventually occupied by the group B aftershocks. It is the increase of the ambient compressive stress in this part of the group B source volume that causes the medium to become less attenuating due to the closure of fluid-filled cracks. Therefore, the aftershocks from that part of the group B source volume tend to give rise to higher coda Q values. This interpretation depends on the validity of the increase of coda Q measurements after the mainshock at depth above 5 km. Judging from the measurement uncertainty, this increase is only marginally significant and further confirmation is needed.

Discussion and Conclusion

The most interesting findings of this study are the two sharp drops in coda Q following the mainshock (Figure 5b). The first sharp drop of coda Q occurred one day after the mainshock and lasted for two days before returning to the background level. The drop is defined by measurements from 46 events. About 60% of these 46 events originates from group B, and 40% of them from group A aftershocks. Focal depths of these 46 events, though concentrated from 5 to 10 km, span the entire depth range from the surface to 20 km. There is no clear correlation of this low coda Q with the spatial distribution of events. A second sharp drop of coda Q occurred six days after the mainshock and lasted for about a day. It is less well-defined, as the drop is determined by only 9 events with large measurement errors. From the plots of focal depth versus coda Q (Figure 6a), it can be seen that a clear decrease of coda Q values has taken place in the source volume as a consequence of the occurrence of the mainshock.

The change of coda Q must be a manifestation of a change of property of the medium, rather than a change of source radiation. The drop of coda Q is likely to be caused by the formation of new cracks and the reopening of existing cracks which, in turn, can be driven by a change in the stress concentration as a consequence of asperity redistribution following the mainshock. Therefore, the measurement of coda Q can be used to infer the subsurface stress conditions. Even though a single crack may have dimensions much smaller than the dominant wavelength, clusterings of cracks may, nevertheless, behave as patches of heterogeneities with characteristic dimension of several hundred meters—thus approaching the wavelength of S waves with the dominant frequency considered here. The rapid drop of coda Q immediately following the mainshock may be caused by an avalanche in the generation of new fluid-filled cracks and the reopening of existing cracks due to the disturbance produced by the mainshock; this condition is further intensified by the rapid occurrences of aftershocks. Through a process of long-term tectonic loading, the response of the source region to a slow increase in the ambient

stress is creep rather than brittle microfractures. However, a sudden decrease of the maximum principal stress (σ_1 in this case approximately along the band of group A aftershocks in Figure 2) due to the occurrences of the mainshock and aftershocks can facilitate tensile failures, especially in regions where the minimum principal stress σ_3 is small. The mainshock and the aftershocks represent a process for the medium to re-establish equilibrium. Following a long period of low level stress buildup, the sudden removal or reduction of the ambient stress field may therefore induce extensive crack opening. In fact, the mainshock and the rapidly occurring aftershocks may have shifted the regional stress concentration to new and nearby locations, one possible location may be the upper part of the group B events. This can be considered as a part of the overall redistribution of asperities in response to the mainshock. There have been active attempts in recent years to model the nucleation, growth, and interaction of microcracks both numerically (NEMAT-NASSER and HORII, 1982; HORII and NEMAT-NASSER, 1985) and analytically (ASHBY and HALLMAN, 1986; SAMMIS and ASHBY, 1986; ASHBY and SAMMIS, 1988). Some of these approaches take into acount the medium heterogeneities. These studies support a model of tensile crack generation and growth due to sudden unloading, and the redistribution of stress concentration due to a sudden change of ambient conditions may lead to a redistribution of crack density. It is within this numerical and analytical framework that the observations of coda Q fluctuations are interpreted. As the drop of the coda Q subsides and returns to the background level, a mechanism of crack closure is likely in operations. Again, we assume that the process of anelasticity attenuation dominates over wave scattering process. If this interpretation is correct, the finding that the process of crack opening and closure can be accomplished so swiftly within days, suggests that rapid state of stress changes are in operation in the source volume following the occurrence of a large earthquake. Accompanying the rapid changes of the ambient stress field, a surge of crack openings and closures may be taking place in the source rupture volume that is reflected by coda Q fluctuations. The present study and those from other investigators (for example, SATO, 1986) have reported fluctuations of coda Q values following large earthquakes. These observations are consistent with the model of stress field disequilibrium during the period of readjusting following the mainshock. Depending on the nature of the readjustment process, multiple occurrences of patches of high crack density within the source volume may result in multiple drops of coda Q. The second drop of coda Q observed in this study, though less reliably determined, could be similarly interpreted. The lack of a large number of foreshocks prevents a detailed definition of coda Q changes immediately before the mainshock. During a 14-day period before the mainshock, three events are found to be located in the source volume. A drop in coda Q is suggested (Figure 5a and events #55 and #57 in Table 1), but the evidence is weak due to the small number of foreshocks.

Acknowledgements

The authors would like to express thanks to F. S. Chang, S. C. Sen, and J. H. Yuh for assistance in data processing. We benefit from illuminating discussions with Charles G. Sammis, and helpful comments from Bob Herrmann and an anonymous reviewer. This study was sponsored by the Academia Sinica, the National Science Council of the Republic of China under Grant No. NSC77-0202-M001-04, and USGS Contract No. 14-08-001-A0264.

REFERENCES

AKI, K. (1969), *Analysis of the seismic coda of local earthquakes as scattered waves*, J. Geophys. Res. *74*, 615–631.

AKI, K. (1980a), *Attenuation of shear-waves in the lithosphere for frequencies from 0.05 to 25 Hz*, Phys. Earth Planet. Inter. *21*, 50–60.

AKI, K. (1980b), *Scattering and attenuation of shear waves in the lithosphere*, J. Geophys. Res. *85*, 6496–6504.

AKI, K. and B. CHOUET (1975), *Origin of coda waves: Source, attenuation, and scattering effects*, J. Geophys. Res. *80*, 3322–3342.

ASHBY, M. F. and S. D. HALLMAN (1986), *The failure of brittle solids containing small cracks under compressive stress state*, Acta Metall. *34*, 497–561.

ASHBY, M. F. and C. G. SAMMIS (1988), *The damage mechanics of brittle solids in compression*, submitted to Acta Metall.

CHEN, K.-C. and J.-H. WANG (1986), *The May 20, 1986 Hualien, Taiwan earthquake and its aftershocks*, Bull. Inst. Earth Sci., Academia Sinica *6*, 1–14.

CHOUET, B. (1976), *Source, scattering, and attenuation effects in high frequency seismic waves*, Ph.D. Thesis, Massachusetts Institute of Technology, Cambridge, Massachusetts.

CHOUET, B. (1979). *Temporal variation in the attenuation of earthquake coda near Stone Canyon, California*, Geophys, Res. Lett. *6*, 143–146.

CHOUET, B., K. AKI, and M. RSUJIURA (1978), *Regional variation of the scaling law of earthquake wave spectra*, Bull. Seismol. Soc. Am. *68*, 49–79.

GUSEV, A. A. and V. K. LEMZIKOV (1985), *Properties of scattered elastics waves in the lithosphere of Kamchatka: Parameters and temporal variation*, Tectonophys. *112*, 137–153.

HERRMANN, R. B. (1980), *Q estimate using the coda of local earthquakes*, Bull. Seismol. Soc. Am. *70*, 447–468.

HORII, H. and S. NEMAT-NASSER (1986), *Brittle failure in compression: Splitting, faulting, and brittle-ductile transition*, Phil. Tran. Roy. Soc. A *319*, 337–374.

HSU, T. L. (1954), *On the geographical features and the recent uplifting movement of the coastal range, eastern Taiwan*, Bull. Geol. Surv. Taiwan *7*, 9–18.

JIN, A. (1981), *Duration of coda waves and the backscattering coefficient*. Paper presented at the Symposium on Seismology in China, State Seismol. Bur., Shanghai, China.

JIN, A. and AKI, K. (1986), *Temporal changes in coda Q before the Tangshan earthquake of 1976 and the Haicheng earthquake of 1975*, J. Geophys. Res. *91*, 665–673.

KOPNICHEV, Y. F. (1977), *The role of multiple scattering in the formation of a seismogram's tail*, Izv. Acad. Aci. USSR Phys. Solid Earth. Engl. Transl. 13, 394–398.

LEE, W. H. K., K. AKI, B. CHOUET, P. JOHNSON, S. MARKS, J. T. NEWBERRY, A. S. RYALL, S. W. STEWART, and D. M. TOTTINGHAM (1986), *A preliminary study of coda Q in California and Nevada*, Bull. Seism. Soc. Am. *76*, 1143–1150.

LIAW, Z.-S., C. WANG, and Y. T. YEH (1986), *A study of aftershocks of the 20 May 1986 Hualien earthquake*, Bull. Inst. Earth Sci., Academia Sinica *6*, 15–27.

NEMAT-NASSER, S. and H. HORII, (1982), *Compression induced nonplanar crack extension with application to splitting, extension, and rockburst*, J. Geophys. Res. *87*, 6805–6821.

NOVELO-CASANOVA, D. A., E. BERG, V. HSU, and C. E. HELSLEY (1985), *Time-space variation seismic S-wave coda attenuation (Q) and magnitude distribution for the Pelatan earthquake*, Geophys. Res. Lett. *12*, 789–792.

PENG, J. Y., K. AKI, B. CHOUET, P. JOHNSON, W. H. K. LEE, S. MARKS, J. T. Newberry, A. S. RYALL, S. W. STEWART, and D. M. TOTTINGHAM (1987), *Temporal change in coda Q associated with the Round Valley, California, earthquake of November 23, 1984*, J. Geophys. Res. *92*, 3507–3526.

RAUTIAN, T. G. and V. I. KHALTURIN (1978), *The use of coda for determination of the earthquake source spectrum*, Bull. Seism. Soc. Am. *68*, 923–940.

SAMMIS, C. G. and M. F. ASHBY (1986), *The failure of brittle porous solids under compressive stress states*, Acta Metall. *34*, 511–526.

SATO, H. (1977), *Energy propagation including scattering effects: Single isotropic scattering approximation*, J. Phys. Earth *25*, 27–41.

SATO, H. (1978), *Mean free path of S-waves under the Kanto district of Japan*, J. Phys. Earth *26*, 185–198.

SATO, H. (1979), *Wave propagation in one-dimensional inhomogeneous elastic media*, J. Phys. Earth *27*, 455–466.

SATO, H. (1984), *Attenuation and envelope formation of three-component seismograms of small local earthquakes in randomly inhomogeneous lithosphere*, J. Geophys. Res. *89*, 1221–1241.

SATO, H. (1986), *Temporal change in attenuation intensity before and after the Eastern Yamanashi earthquake of 1983 in central Japan*, J. Geophys. Res. *91*, 2049–2061.

SHIN, T.-C., W.-J. SU, and P.-L. LEU (1987), *Coda-Q estimates for Taiwan Area*, Bull. Geophys., Natl. Central Univ. *27/28*, 95–110.

SINGH, S. and R. HERRMANN (1983), *Regionalization of crustal coda Q in the continental United States*, J. Geophys. Res. *88*, 527–538.

TSAI, Y. B., T. L. TENG, J. M. CHIU, and H. L. LIU (1977), *Tectonic implications of seismicity in the Taiwan region*, Mem. Geol. Soc. China *2*, 13–41.

TSUJIURA, M. (1978), *Spectral analysis of the coda waves from local earthquakes*, Bull. Earthq. Res. Inst., Univ. Tokyo. *53*, 1–48.

TSUKUDA, T. (1985), *Coda Q before and after a medium-scale earthquake*, Paper presented at the 23rd General Assembly, Int. Assoc. of Seismol. and Phys. of the Earth's Inter., Tokyo, Japan.

WANG, J. H., C. C. LIU, K. C. CHEN, and Y. S. CHENG (1985), *Taiwan Telemetered Seismographic Network* (in Chinese). Proc. Seminar Commemor. 50th Anniver. Great Hsinchu-Taichung Earthq., 1935, 124–136.

WU, R. S. (1984), *Seismic wave scattering and the small-scale inhomogeneities in the lithosphere*, Ph.D. Thesis, Mass. Inst. of Technol., Cambridge, Mass., U.S.A.

WYSS, M. (1985), *Precursors to large earthquakes*, Earthq. Predict. Res. *3*, 519–543.

(Received August 29, 1988, revised/accepted November 14, 1988)